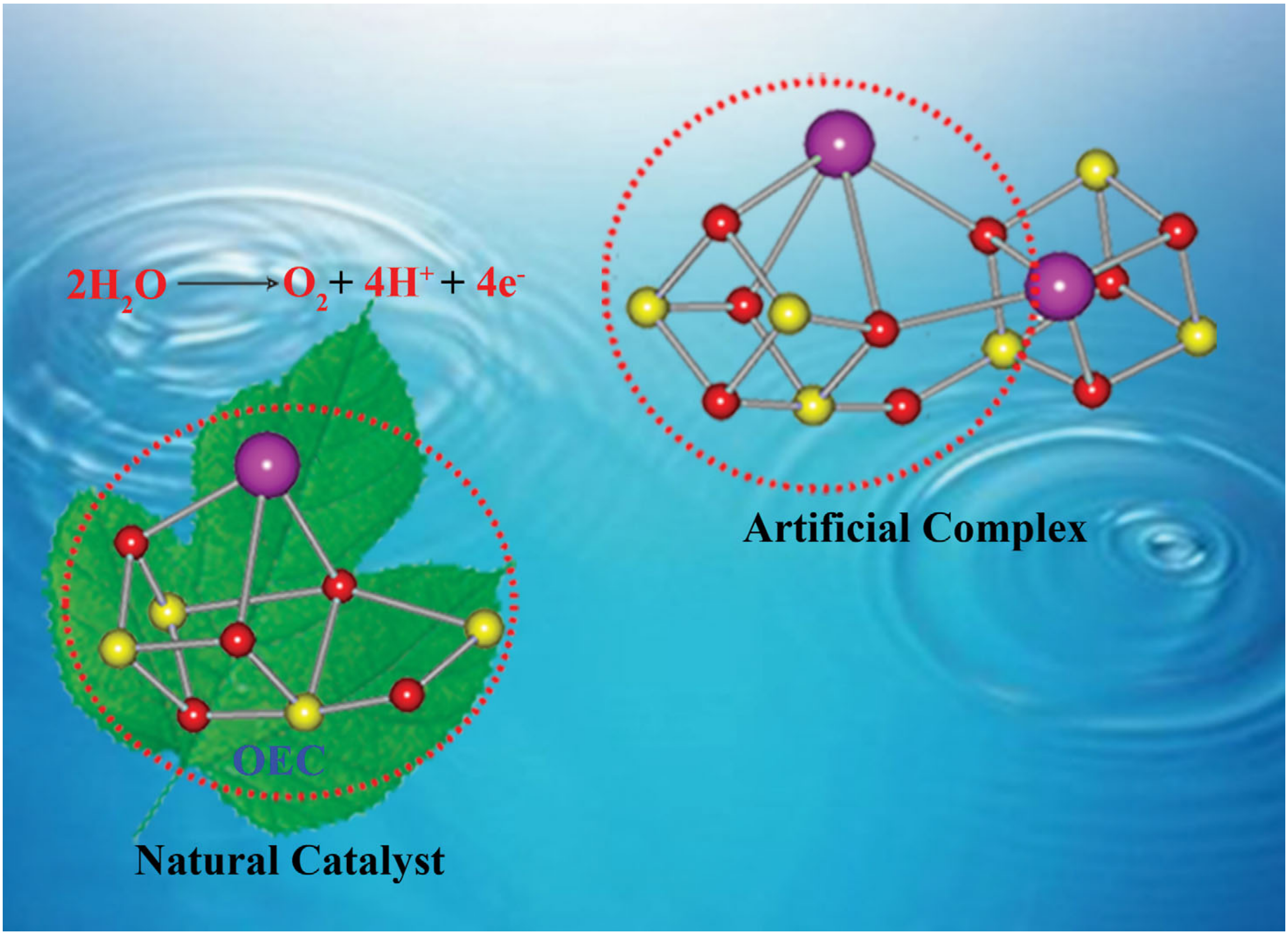

Showcasing work from the Laboratory of Hongxing Dong, Polymer Materials Research Center, College of Materials Science and Chemical Engineering, Harbin Engineering University (Harbin) and Laboratory of Chunxi Zhang, Laboratory of Photochemistry, Institute of Chemistry, Chinese Academy of Sciences (Beijing).

A synthetic model for the oxygen-evolving complex in Sr^{2+}-containing photosystem II

It is of a great challenge for chemists to synthesize accurate structural model for the oxygen-evolving complex (OEC) in Photosystem II. Here, a novel artificial complex is synthesized with remarkable structural similarities to the OEC, in respects of the peripheral ligands, the Mn_3SrO_4 cuboidal moiety and three different types of bridging oxido moieties, which may provide new insights to understanding of the structure and properties of the OEC in nature.

As featured in:

See Chunxi Zhang,
Hongxing Dong *et al.*,
Chem. Commun., 2014, **50**, 9263.

ChemComm

COMMUNICATION

View Article Online
View Journal | View Issue

A synthetic model for the oxygen-evolving complex in Sr^{2+}-containing photosystem II†

Changhui Chen,[a] Chunxi Zhang,*[b] Hongxing Dong*[a] and Jingquan Zhao[b]

Cite this: *Chem. Commun.*, 2014, 50, 9263

Received 30th March 2014,
Accepted 25th April 2014

DOI: 10.1039/c4cc02349h

www.rsc.org/chemcomm

A novel heterometallic MnSr complex containing the Mn_3SrO_4 cuboidal moiety and all types of μ-O^{2-} moieties observed in the oxygen-evolving complex (OEC) in Sr^{2+}-containing photosystem II (PSII) has been synthesized and characterized, which provides a new synthetic model of the OEC.

The oxygen-evolving complex (OEC) within photosystem II (PSII) of plants, algae and cyanobacteria serves as nature's blueprint for a water splitting catalyst.[1,2] The structure of OEC has been recently revealed by the X-ray crystal structure of PSII (Fig. 1).[3–5] There are two unique characteristics of the structural motif of OEC. One is the incorporation of Ca^{2+} within the Mn_3CaO_4 cubane through three μ-oxido moieties. The other is the simultaneous presence of μ_2-O^{2-} (*e.g.* O4), μ_3-O^{2-} (*e.g.* O1, O2, O3) and μ_4-O^{2-} (*e.g.* O5). The entire OEC is embedded in a large protein matrix through H-bond interactions and direct ligations to six carboxylate and one imidazole group of the amino acid residues on the D_1 and CP_{43} polypeptides in PSII. Ca^{2+} is known to be an essential component of the function of OEC,[6] which can be functionally replaced only by Sr^{2+} without significantly disturbing the structure of the OEC.[5,7]

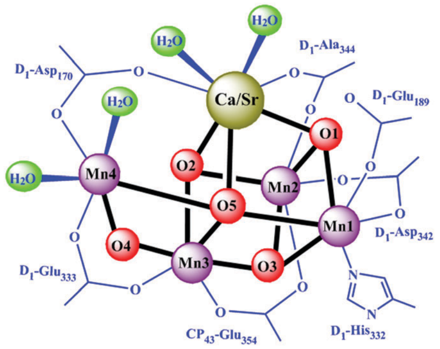

Fig. 1 Scheme for the OEC in PSII.

The water-splitting reaction involves five different S-states (S_n, n = 0 to 4) of the OEC. Spectroscopic studies have shown that the oxidation states and the geometry of the OEC undergo changes during these state transitions.[8,9] However, the detailed catalytic mechanism of the OEC, including the role of Ca^{2+}/Sr^{2+} in PSII remains under extensive debate.[10–17] Due to the structural complexity of the OEC, it is a great challenge for chemists to synthesize accurate structural and functional models for the OEC in the laboratory.

To date, many multinuclear Mn complexes have been synthesized as models of the OEC.[1,18–23] However, only a few synthetic MnCa and MnSr heterometallic complexes[24–36] have been reported. Moreover, no effort has been made to mimic the three types of bridging oxido moieties (μ_2-O^{2-}, μ_3-O^{2-} and μ_4-O^{2-}) at the same time. In terms of the functional properties, the redox potentials of the two current complexes containing $Mn^{IV}{}_3CaO_4$ or $Mn^{IV}{}_3SrO_4$ cuboidal moieties with a multinucleating ligand[34,36] were very low, −0.5V *vs.* NHE, compared to the requirement of the thermodynamic potential for water oxidation (+0.8 V *vs.* NHE).[37,38] Therefore, it is highly desirable to synthesize more accurate structural and functional models for the OEC.

Here, we report a novel MnSr complex containing the Mn_3SrO_4 cuboidal moiety and all types of μ-oxido moieties observed in the OEC; in addition, the complex exhibits the redox potential at +0.9 V *vs.* NHE, suggesting its potential as a good synthetic model for the OEC.

This complex was synthesized in a reaction of $Bu^n{}_4NMnO_4$, $Mn(CH_3CO_2)_2(H_2O)_4$ and $Sr(CH_3CO_2)_2(H_2O)_{0.5}$ in a molar ratio of 4 : 1 : 1 in boiling acetonitrile in the presence of an excess of pivalic acid. Red-brown crystals were formed after cooling, which were further recrystallized in ethyl acetate solution in

---

[a] *Polymer Materials Research Center, Key Laboratory of Superlight Materials & Surface Technology of Ministry of Education, College of Materials Science and Chemical Engineering, Harbin Engineering University, Harbin 150001, China. E-mail: dhongxing@hrbeu.edu.cn; Tel: +86-451-82568191*

[b] *Laboratory of Photochemistry, Institute of Chemistry, Chinese Academy of Sciences, Beijing 100190, China. E-mail: chunxizhang@iccas.ac.cn; Fax: +86-10-82617315; Tel: +86-10-82617053*

† Electronic supplementary information (ESI) available: Experimental section, X-ray structure information, BVS calculations, UV-vis absorption spectrum, EPR spectrum, Cyclic voltammogram (CV), Differential pulse voltammogram (DPV). CCDC 994140. For ESI and crystallographic data in CIF or other electronic format see DOI: 10.1039/c4cc02349h

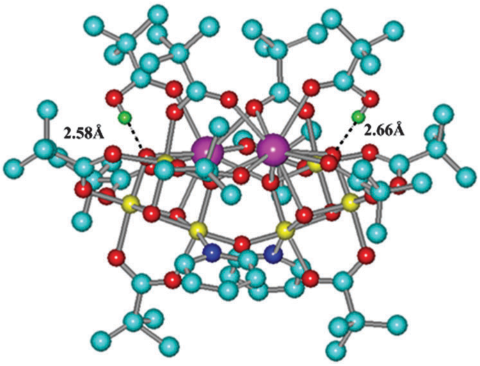

Fig. 2 The structure of complex **1**. Mn, Sr, O, N, C and H are shown in yellow, violet, red, blue, cyan and green, respectively. For clarity, all hydrogen atoms except two active protons of pivalic acids are omitted. H-bonds are shown with a dashed line, and values display the H-bond lengths.

the presence of ∼2% pyridine (for details of preparation, see ESI†). The final product of complex **1**, $[\mathrm{Mn^{IV}}_6\mathrm{Sr_2O_9(Bu^{\mathit{t}}CO_2)_{10}(Bu^{\mathit{t}}CO_2H)_2(C_5H_5N)_2}]$ was obtained as black rod crystals with a yield of 22% (on a strontium basis).‡

Fig. 2 shows the crystal structure of complex **1**. The peripheral ligands of complex **1** include ten pivalate, two pivalic acid and two pyridine groups. Each coordinated pivalic acid further interacts with μ_3-O^{2-} through a strong H-bond (Fig. S2, ESI†). All these ligations and H-bond interactions in complex **1** are reminiscent of the protein environment of the OEC in PSII.[3–5]

All six Mn ions are six-coordinate. The two Sr^{2+} ions are eight- and nine-coordinate, respectively, resulting in the asymmetry of the entire structure of complex **1** (Table S3, ESI†).

In the core of complex **1** (Fig. 3), two $\mathrm{Mn^{IV}}_3\mathrm{SrO_4}$ cuboidal units are connected by one μ_2-O^{2-} and two μ_4-O^{2-} moieties. Three types of μ-O^{2-} moieties (μ_2-O^{2-}, μ_3-O^{2-}, μ_4-O^{2-}) are seen in complex **1**. The +4 valences of all six Mn ions and the doubly deprotonated state of all bridged oxygen atoms are confirmed by bond-valence sum calculations (Table S4, ESI†). To our knowledge, this is the first time that a MnSr complex containing three types of μ-O^{2-} moieties simultaneously has been synthesized. Therefore, complex **1** provides an artificial model to interrogate the functionalities of these μ-O^{2-} moieties in the OEC of PSII.

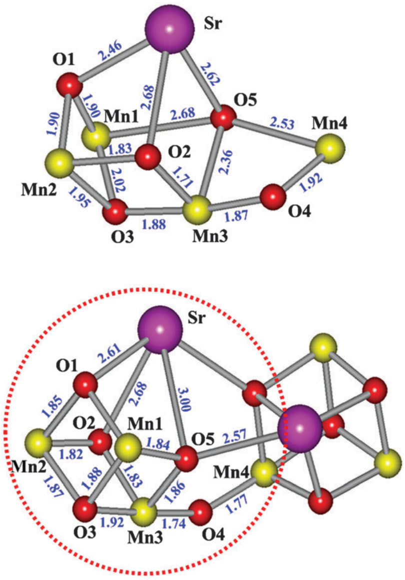

Fig. 3 The core of complex **1** (bottom) and OEC in PSII (top). The fraction of Mn_4SrO_5 of complex **1** similar to the OEC is emphasized with a red-dashed circle. The values display the lengths of selected bonds (Å).

The average distance of Mn–Sr in complex **1** is 3.58 Å, which is longer than 3.40 Å observed in a previous Mn_3SrO_4 complex containing a multinucleating ligand,[34] but is close to the 3.55 Å separation observed in OEC of Sr^{2+}-containing PSII[5] (Table S5, ESI†). The average 2.77 Å distance of Mn–Mn in complex **1** is slightly shorter than that observed previously in the Mn_3SrO_4 complex[34] (2.82 Å), and also obviously shorter than 3.00 Å than that in the OEC of Sr^{2+}-containing PSII,[5] which is likely because of the higher oxidation states of the Mn ions in complex **1**.

The average distance of μ_3-O–Mn in the complex **1** is 1.86 Å, which is slight shorter than 1.88 Å observed in the OEC of Sr^{2+}-containing PSII,[5] or 1.87 Å in the Mn_3SrO_4 complex reported.[34] The average distance of μ_2-O–Mn in complex **1** is 1.76 Å, which is shorter than 1.89 Å observed in OEC of Sr^{2+}-containing PSII[5] (Table S5, ESI†), which is likely because of the higher oxidation state of the Mn ions in complex **1** as well.

The lengths of the two μ_4-O–Mn in complex **1** are in the range of 1.84 Å to 1.87 Å with an average of 1.86 Å, which is a common distance for μ_4-O^{2-}–Mn in most multinuclear Mn complexes and heteronuclear MnSr or MnCa complexes.[24,25,35,39] However, the length of 1.86 Å is remarkably shorter (by 0.64 Å) than the average value of 2.5 Å in the OEC of Ca^{2+} or Sr^{2+} containing PSII.[4,5] It is important to point out that the μ_4-O5 atom in the OEC has attracted extensive attention in the studies of water oxidation in PSII recently.[14,16,17,39–43] Theoretical studies[16,17] have suggested that the μ_4-O5 atom may act as a source of oxygen atoms for the formation of O–O bonds in the higher S-state (*e.g.* S_3, S_4) of the OEC, in which the valences for all Mn ions are most likely to be +4,[8,9] similar to that in complex **1**. It is important to mention that the assignment of this μ_4-O5 atom was not unambiguous due to its much weaker electron density than all other bridging oxido moieties in the X-ray diffraction data of the OEC.[4,5,39] The structural characteristics of the μ_4-O^{2-} in complex **1** and various MnSr–MnCa complexes[24,25,35] could be considered as structural pieces of evidence to argue that the binding and the function of the μ_4-O5 atom in the OEC is worth being addressed in the future.

The EPR measurements show that complex **1** displays similar EPR signals as observed in the $Mn_3Ca_2O_4$ complex reported by Christou's group.[35] It was found that both solid and solution samples of complex **1** give rise to similar EPR signals (Fig. S5, ESI†), which suggests that the entire structure of complex **1** is maintained not only in crystals but also in solution.

Cyclic voltammogram (CV) measurements (Fig. 4) of complex **1** display two irreversible redox processes at −0.5 V and +0.9 V *vs.* NHE, assigned to the couples of $[\mathrm{Mn^{III}Mn^{IV}}_2\mathrm{SrO_4}]/[\mathrm{Mn^{IV}}_3\mathrm{SrO_4}]$ and $[\mathrm{Mn^{IV}}_3\mathrm{SrO_4}]/[\mathrm{Mn^{V}Mn^{IV}}_2\mathrm{SrO_4}]$, respectively, according to a previous report.[34,44] The irreversibility of these two couples may reflect some structural changes during the redox processes. It is noticed that the +0.9 V redox process appears only after undertaking the −0.5 V irreversible redox process (Fig. S6 and S7, ESI†), suggesting

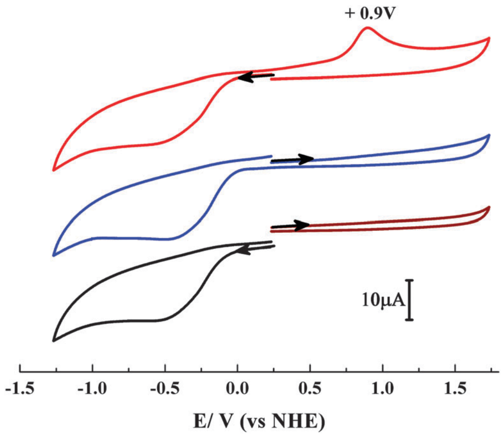

Fig. 4 Cyclic voltammogram of complex **1** in a 3 : 2 ratio of $EtCl_2$–ethyl acetate. Potentials are referenced to NHE. Scan rate: 100 mV s^{-1}, arrows display the scan direction.

that the occurrence of the former requires the structural change taking place during the redox process of the latter. Interestingly, the +0.9 V redox potential was not observed in previous $Mn^{IV}{}_3CaO_4$ or $Mn^{IV}{}_3SrO_4$ complexes,[34,36] while it is close to the +0.8 V to +0.9 V *vs.* NHE redox potential[37,38] of the OEC in PSII.

In summary, a new complex has been synthesized with remarkable structural similarities to the OEC in Sr^{2+}-containing PSII, with respect to the peripheral ligands, the Mn_3SrO_4 cuboidal moiety, and the three different types of bridging oxido moieties at the same time. The redox characteristics of this new complex are close to that of the OEC as well. Therefore, complex **1** may serve as a highly accurate synthetic model of the OEC in PSII, which may provide new insights into the understanding of the structure and properties of the OEC in nature.

This work was supported by the National Natural Science Foundation of China (No. 20973186 and 31070216) and the Fundamental Research Funds for the Central Universities of China (No. HEUCFT1009, HEUCF201403008).

Notes and references

‡ Elemental analysis (%) calcd for complex **1** ($C_{70}H_{120}N_2O_{33}Mn_6Sr_2$): C, 41.57; H, 5.98; N, 1.38; found: C, 41.57; H, 5.79; N, 1.63. Crystal structure data for complex **1:** $C_{70}H_{120}N_2O_{33}Mn_6Sr_2$, $M = 2022.56$, black rod crystal, orthorhombic, $P2_12_12_1$, $a = 15.290(3)$ Å, $b = 18.205(4)$ Å, $c = 36.041(7)$ Å, $\alpha = 90.00°$, $\beta = 90.00°$, $\gamma = 90.00°$, $V = 10032(3)$ Å^3, 32 066 reflections collected; 1083 parameters were refined in the final cycle of refinement using 17 540 reflections ($I > 2\sigma(I)$); $R_1 = 0.0947$, $wR_2 = 0.2202$ (based on F^2 and all data). Also see CCDC 994140 for complex **1**.

1 J. P. McEvoy and G. W. Brudvig, *Chem. Rev.*, 2006, **106**, 4455–4483.
2 J. Barber, *Chem. Soc. Rev.*, 2009, **38**, 185–196.
3 K. N. Ferreira, T. M. Iverson, K. Maghlaoui, J. Barber and S. Iwata, *Science*, 2004, **303**, 1831–1838.
4 Y. Umena, K. Kawakami, J.-R. Shen and N. Kamiya, *Nature*, 2011, **473**, 55–60.
5 F. H. M. Koua, Y. Umena, K. Kawakami and J. R. Shen, *Proc. Natl. Acad. Sci. U. S. A.*, 2013, **110**, 3889–3894.
6 C. F. Yocum, *Coord. Chem. Rev.*, 2008, **252**, 296–305.
7 N. Cox, L. Rapatskiy, J. H. Su, D. A. Pantazis, M. Sugiura, L. Kulik, P. Dorlet, A. W. Rutherford, F. Neese, A. Boussac, W. Lubitz and J. Messinger, *J. Am. Chem. Soc.*, 2011, **133**, 3635–3648.
8 H. Dau and M. Haumann, *Coord. Chem. Rev.*, 2008, **252**, 273–295.
9 K. Sauer, J. Yano and V. K. Yachandra, *Coord. Chem. Rev.*, 2008, **252**, 318–335.
10 V. L. Pecoraro, M. J. Baldwin, M. T. Caudle, W. Y. Hsieh and N. A. Law, *Pure Appl. Chem.*, 1998, **70**, 925–929.
11 M. Lundberg and P. E. M. Siegbahn, *Phys. Chem. Chem. Phys.*, 2004, **6**, 4772–4780.
12 J. P. McEvoy and G. W. Brudvig, *Phys. Chem. Chem. Phys.*, 2004, **6**, 4754–4763.
13 W. Ames, D. A. Pantazis, V. Krewald, N. Cox, J. Messinger, W. Lubitz and F. Neese, *J. Am. Chem. Soc.*, 2011, **133**, 19743–19757.
14 M. Kusunoki, *J. Photochem. Photobiol., B*, 2011, **104**, 100–110.
15 H. Dau, I. Zaharieva and M. Haumann, *Curr. Opin. Chem. Biol.*, 2012, **16**, 3–10.
16 H. Isobe, M. Shoji, S. Yamanaka, Y. Umena, K. Kawakami, N. Kamiya, J. R. Shen and K. Yamaguchi, *Dalton Trans.*, 2012, **41**, 13727–13740.
17 P. E. M. Siegbahn, *Biochim. Biophys. Acta*, 2013, **1827**, 1003–1019.
18 E. Y. Tsui, J. S. Kanady and T. Agapie, *Inorg. Chem.*, 2013, **52**, 13833–13848.
19 C. Herrero, B. Lassalle-Kaiser, W. Leibl, A. W. Rutherford and A. Aukauloo, *Coord. Chem. Rev.*, 2008, **252**, 456–468.
20 C. S. Mullins and V. L. Pecoraro, *Coord. Chem. Rev.*, 2008, **252**, 416–443.
21 S. Mukhopadhyay, S. K. Mandal, S. Bhaduri and W. H. Armstrong, *Chem. Rev.*, 2004, **104**, 3981–4026.
22 G. C. Dismukes, R. Brimblecombe, G. A. N. Felton, R. S. Pryadun, J. E. Sheats, L. Spiccia and G. F. Swiegers, *Acc. Chem. Res.*, 2009, **42**, 1935–1943.
23 M. D. Kärkäs, E. V. Johnston, O. Verho and B. Åkermark, *Acc. Chem. Res.*, 2014, **47**, 100–111.
24 A. Mishra, W. Wernsdorfer, K. A. Abboud and G. Christou, *Chem. Commun.*, 2005, 54–56.
25 A. Mishra, J. Yano, Y. Pushkar, V. K. Yachandra, K. Abboud and G. Christou, *Chem. Commun.*, 2007, 1538–1540.
26 I. J. Hewitt, J. K. Tang, N. T. Madhu, R. Clerac, G. Buth, C. E. Anson and A. K. Powell, *Chem. Commun.*, 2006, 2650–2652.
27 S. Nayak, H. P. Nayek, S. Dehnen, A. K. Powell and J. Reedijk, *Dalton Trans.*, 2011, **40**, 2699–2702.
28 Y. J. Park, J. W. Ziller and A. S. Borovik, *J. Am. Chem. Soc.*, 2011, **133**, 9258–9261.
29 E. Y. Tsui, R. Tran, J. Yano and T. Agapie, *Nat. Chem.*, 2013, **5**, 293–299.
30 N. Li, M. Wang, C. B. Ma, M. Q. Hu, R. W. Zhou, H. Chen and C. N. Chen, *Inorg. Chem. Commun.*, 2010, **13**, 730–732.
31 L. B. Jerzykiewicz, J. Utko, M. Duczmal and P. Sobota, *Dalton Trans.*, 2007, 825–826.
32 E. S. Koumousi, S. Mukherjee, C. M. Beavers, S. J. Teat, G. Christou and T. C. Stamatatos, *Chem. Commun.*, 2011, **47**, 11128–11130.
33 A. Mishra, Y. Pushkar, J. Yano, V. K. Yachandra, W. Wernsdorfer, K. A. Abboud and G. Christou, *Inorg. Chem.*, 2008, **47**, 1940–1948.
34 E. Y. Tsui and T. Agapie, *Proc. Natl. Acad. Sci. U. S. A.*, 2013, **110**, 10084–10088.
35 S. Mukherjee, J. A. Stull, J. Yano, T. C. Stamatatos, K. Pringouri, T. A. Stich, K. A. Abboud, R. D. Britt, V. K. Yachandr and G. Christou, *Proc. Natl. Acad. Sci. U. S. A.*, 2012, **109**, 2257–2262.
36 J. S. Kanady, E. Y. Tsui, M. W. Day and T. Agapie, *Science*, 2011, **333**, 733–736.
37 H. Dau and I. Zaharieva, *Acc. Chem. Res.*, 2009, **42**, 1861–1870.
38 I. Vass and S. Styring, *Biochemistry*, 1991, **30**, 830–839.
39 Y. Wang, C. Zhang, L. Wang and J. Zhao, *Chin. Sci. Bull.*, 2013, **58**, 3213–3216.
40 D. A. Pantazis, W. Ames, N. Cox, W. Lubitz and F. Neese, *Angew. Chem., Int. Ed.*, 2012, **51**, 9935–9940.
41 P. Gatt, S. Petrie, R. Stranger and R. J. Pace, *Angew. Chem., Int. Ed.*, 2012, **51**, 12025–12028.
42 L. Rapatskiy, N. Cox, A. Savitsky, W. M. Ames, J. Sander, M. M. Nowaczyk, M. Rögner, A. Boussac, F. Neese, J. Messinger and W. Lubitz, *J. Am. Chem. Soc.*, 2012, **134**, 16619–16634.
43 C. Glöckner, J. Kern, M. Broser, A. Zouni, V. Yachandra and J. Yano, *J. Biol. Chem.*, 2013, **288**, 22607–22620.
44 C. E. Dube, S. Mukhopadhyay, P. J. Bonitatebus, R. J. Staples and W. H. Armstrong, *Inorg. Chem.*, 2005, **44**, 5161–5175.